INCREASINGLY UNDULATORY JET STREAMS

Stephen R. Mullens*
Norman, Oklahoma

1. INTRODUCTION

Changes in the characteristics of the midlatitude jet stream have been noted in response to anthropogenic climate change. The poleward movements of both northern (NH) and southern hemispheric (SH) jets have been detected through analysis of satellite observations (Yin 2005), radiosonde data and reanalyses (Marshall 2003), and predicted to continue in global climate models (Arblaster and Meehl 2006, Miller et al 2006). Hypothesized causes of this poleward movement have included a shift in the region of strongest baroclinicity due to Arctic Amplification (Rinke and Dethloff 2008), an increase in the eddy length scale (Kidston et al. 2011), an increase in anticyclonic wave breaking (Rivière 2011), a decrease in the dry static stability (Yin 2005), and an increase in latent heat release (Laîné et al. 2009).

The zonal-mean zonal wind of SH westerlies have been observed to increase in strength in reanalyses (Chen and Held 2007), and are likely to continue to increase in response to greenhouse gas forcing (Barnes and Polvani 2013). Conversely, the NH zonal-mean zonal wind has not been observed to change, though it may weaken with increasing Arctic Amplification (Serreze and Barry 2011). Importantly, the magnitude of these global changes has been shown to be both model and regionally dependent (Ihara and Kushnir 2009, Rinke and Dethloff 2008, Woolings and Blackburn 2012).

The 500 hPa isoheight associated with the largest latitudinal extent of Rossby waves has been shown to have increased with time (Barnes 2013). This is likely related to an increase in the tropopause height (Lorenz and DeWeaver 2007, Yin 2005).

Although the characteristics and sources of changes in jet latitude, speed, and height have been sought, those of jet undulation and its changes have yet to be determined. Barnes (2013) and Screen and Simmonds (2013) show that changes in jet amplitude are limited in statistical significance to a few regions and seasons, and that these changes are complicated by the applied jet stream definition used. It would appear that a lack of amplification change would imply a lack of change in the characteristics of jet stream undulance. Previous studies of jet amplitude have involved following particular 500 hPa isoheights by day or by season to characterize the jet stream, with the heights used varying by season. Using isoheights may not accurately capture the nature of the jet stream (Barnes 2013). The characteristic high wind speeds of jet streams are associated with large height gradients and not by particular isoheights on constant pressure surfaces. Thus, although jet stream winds are typically geostrophic and are oriented parallel to isoheights, characterizing the jet through isoheights may not accurately identify the highest jet wind speeds.

Although previous studies have not observed significant changes in the amplitude of synoptic-scale waves, the climatological jet stream undulance is independent of the climatological wave amplitude. This study aims to quantify the characteristics and changes in the undulance of the jet stream in both the NH and SH. Identifying the jet stream by its wind speed attempts to avoid the previous definitional difficulties mentioned above.

2. METHODOLOGY

2.1. Data and Regions

Historical jet stream undulance and its changes are examined using the 4-times daily output from the National Center for Environmental Prediction (NCEP)/National Center for Atmospheric Research (NCAR) Reanalysis (Kalnay et al. 1996) between 1948 and 2013. To focus on the upper level jet stream, the 250 hPa and 500 hPa pressure levels are analyzed.

To examine synoptic-scale (or transient eddy) wave patterns, regions are chosen to be similar to a size familiar to operational synoptic-scale forecasting. Six regions of identical size are used, with each region covering an area of 50^{o} latitude by 110^{o} longitude (Table 1). Each region extends to cover the mid-latitudes and is approximately 1.7 times the Rossby wavelength (~5200 km) in longitudinal extent.

Because the impacts of weather and the implications of its changes are most felt over land, each region is centered on commonly identified land regions. The latitudinal extent of each region is large enough to allow for jet streams to wander equatorward and poleward from a more strict definition of the mid-latitudes while still avoiding major polar and tropical related circulations. The longitudinal extent of each region is large enough to include multiple synoptic-scale waves in a single region, thereby capturing the undulant nature of the larger wave pattern and avoiding focus on individual waves. By examining the patterns through several regions, a sense of the regional variability of the characteristics and any changes in jet stream undulance can be gained.

2.2. Symmetric Ratio Equation

The undulant nature of the jet stream within a region is quantified through

* *Corresponding author contact*: Stephen R. Mullens, email: stephen.r.mullens@gmail.com

$$\frac{V-wind}{U-wind}_{symmetric} = \begin{cases} \frac{\sum |v_{ij}|}{\sum |u_{ij}|} - 1 & \text{if } \sum |u_{ij}| > \sum |v_{ij}| \\ 1 - \frac{\sum |u_{ij}|}{\sum |v_{ij}|} & \text{if } \sum |v_{ij}| > \sum |u_{ij}| \end{cases} \quad (1)$$

where u_{ij} and v_{ij} are the u-wind and v-wind components, respectively, at grid point (i, j) at a specified pressure level. To assure the jet stream is identified, only the components from vector wind speeds greater than or equal to 20 ms^{-1} are included in the calculation. Although setting a minimum threshold aligns with customary practice, including all data produces similar results (not shown). The zonal (meridional) nature of the wave pattern at each time is captured in a sum of the absolute value of the u-wind (v-wind) components of each grid location in the region. The absolute values prevent the easterly and westerly (or northerly and southerly) components of waves from summing to zero. Although a minimum speed threshold has been applied, the strength of the wind components are maintained to assure the jet stream is favored over other minor circulations. This is especially valuable when the region is dominated by vector wind speeds above the minimum threshold.

The ratio of the wind components serves to quantify the undulant nature of the jet stream at a particular time. The ratio can be easily conceptualized in that perfectly zonal (meridional) flow results in the absence of any v-wind (u-wind) components, leading to opposing extremes of the ratio spectrum. Uniform southwesterly flow across the region results in equal values of the sum of the components and, thus, a ratio of 1.

Ratios suffer from an asymmetric nature in that comparatively large denominators (numerators) result in ratios ranging from zero to one (one to infinity). Equation 1 is of a form that assures the resulting ratios are of a symmetric nature. Using this 'symmetric ratio,' comparatively large u-wind (v-wind) sums result in ratios ranging from negative one to zero (zero to positive one). Thus, predominately zonal (meridional) flow results in a negative (positive) symmetric ratio, with predominately meridional flow interpreted to be a highly undulant jet stream within the background zonal flow. In this way, the continuous spectrum of possibilities can be easily visualized. Figure 1 provides examples of a range of historical patterns and their resulting symmetric ratios. These patterns represent the minimum (1a; symmetric ratio=-0.84), median (1b; symmetric ratio=-0.43), mean (1c; symmetric ratio=-0.37), and maximum (1d; symmetric ratio=0.24) symmetric ratios found in the North American region at 250 hPa. Thus, the jet stream represented in each successive panel is progressively more undulant.

The symmetric ratio benefits from avoiding analysis of individual waves across daily or seasonal time periods. It is also independent of any climatic changes in jet latitude, speed, width, or characteristic isoheight along a pressure surface. While the polar jet is expected to dominate the observed maximum winds in these regions, subtropical jets are also included in the analysis and no attempt is made to differentiate between them.

The symmetric ratio is calculated for each time in the dataset at a particular pressure level, which can be easily visualized as a time series (Figure 2). Using these values, a histogram of ratios is computed for each year. The symmetric ratios at each time are rounded to the nearest hundredth such that the resulting histograms contain 201 bins. The annual frequency of each ratio can then be plotted with time. A linear rate of change in the annual frequency of each symmetric ratio is computed using linear regression analysis. Multiplying the resulting linear rate by 100 results in units of frequency per century. The changes are smoothed with a 9-ratio centered average. For example, the 9-ratio centered average at 0.05 is the average rates of linear change for symmetric ratios 0.01 through 0.09.

3. RESULTS

As expected, the histograms of symmetric ratios in all regions at 250 hPa are predominately negative, reflecting the prevailing westerlies (Figure 3). They are also normally distributed, reflecting the randomness of the data. The largest histogram spreads are in the NH, likely due to a greater influence from terrain.

At 250 hPa, all regions show increasing (decreasing) frequency of comparatively larger (smaller) symmetric ratios. The change from decreasing to increasing linear trends occurs near the histogram median in each region. Thus, with the median symmetric ratio as the threshold, there exists a clear trend of predominately meridional (zonal) patterns occurring with increasing (decreasing) frequency with time. Thus, the jet stream has become increasingly undulant with time.

The above trend is supported through an analysis of the linear changes in annual symmetric ratio frequencies (Figure 4). For each region, the total frequency of the nine ratios included in the largest linear increase and linear decrease in the 9-ratio centered average is plotted with its linear trend. In each region, the raw data reveals itself to be qualitatively linear, with the linear signals appearing to be greater than their respective internal variations.

At 500 hPa (Figure 5), histograms of the symmetric ratios in all regions are similar to 250 hPa in showing the prevailing westerlies, as expected. The spread of the histograms is increased in all regions, mostly in the meridional direction. This likely reflects the influence of smaller thermal wind values on the jet stream as the atmospheric flow transitions from closed circulations in the lower troposphere to open waves in the upper troposphere. As at 250 hPa, NH histograms show a greater spread in observed symmetric ratios than the SH.

Interestingly, both the North American and European regions show only small linear changes in the frequency of all symmetric ratios. These regions do not clearly show the increasing (decreasing) frequency of meridional (zonal) patterns. All other regions clearly show the qualitative increase in jet stream undulance identified at 250 hPa. South America is also noted as showing a greater reduction in its 500 hPa trend of increasing jet stream undulance compared to its 250 hPa trend than in other SH regions.

To help address the discrepancy between the changes observed in the North American and European regions at 500 hPa and 250 hPa, the characteristics and changes in jet stream undulance are computed for these regions at 400 hPa and 300 hPa (Figure 6). In both regions, the trend of increasingly (decreasing) frequent meridional (zonal) patterns becomes qualitatively more clear and amplified with height.

4. DISCUSSION

4.1 250 hPa jet undulation changes

The symmetric ratios representing meridional (zonal) wave patterns at 250 hPa appear to have occurred with increasing (decreasing) frequency over time in all regions. Thus, the synoptic-scale jet stream is observed to be increasingly undulant with time. This has implications for the provision of upper-level support for surface-based extratropical cyclones and their resulting impacts on extreme weather and climate.

The global increase in jet stream undulance shows hemispheric variation. The largest linear changes in individual symmetric ratio annual frequencies are greater in the SH. However, the NH (SH) changes are spread across (confined to) a greater (lesser) range of symmetric ratios. Because the same amount of data is collected for each year, a sum of the rates of increase across all ratios is equivalent to their sum of the rates of decrease in all regions. Thus, using the regional median symmetric ratio as the threshold, the sum of either the frequency increases or decreases indicate the cumulative linear change of zonal to meridional undulations patterns each year (Table 2). By this method, the SH regions are observed to have undergone approximately twice the change in jet stream undulance as NH regions.

4.2 NH 500 hPa jet undulation changes

Greater regional differences exist between the changes in jet stream undulance at 500 hPa. The changes in all regions are damped from those at 250 hPa, but some regions are damped more than others. The damping or absence of increasing (decreasing) meridional (zonal) patterns seen at 250 hPa appears at first to be influenced by orography. Woolings and Blackburn (2012) expands on the possibilities by postulating that the jet stream in the North Atlantic may respond differently to forcing due to influences from the location of land, orography, and patterns of sea surface temperatures. Why are the North American and European regions dampened so much that the pattern of jet undulation change is small or nonexistent? Why do other regions maintain their jet undulation changes seen aloft?

The differences between NH histogram spread at both 250 hPa and 500 hPa can be explained by the climatological NH storm tracks. Wilson et al. (2009) summarize that in East Asia, the Asian continent disrupts waves upstream. The Tibetan Plateau acts to establish stationary waves downstream that encourage the development of synoptic waves (termed transient eddies by Wilson et al [2009]). This development encourages a greater frequency of meridional patterns than would otherwise occur. The cyclones that develop in the west Pacific continue to the eastern Pacific Ocean until the North American continent disrupts them. Downstream of the continent, new cyclones develop. Higher frequencies of undulant jet stream patterns occur in the North American region due to the presence of both decaying and developing cyclones. Finally, Europe receives the mature cyclones from the Atlantic Ocean that continue well inland before their disruption, leading to the highest frequency of the most undulant jet streams of any NH region.

The causes of the reduction of linear changes are more difficult to discern. Because the pattern of increasing jet stream undulance becomes stronger with height, the reduction must involve an interaction with lower-tropospheric forcing.

It is notable that the Rocky Mountains in North America and the Tibetan Plateau in East Asia are in similar locations within their region. Wilson et al. (2009) sheds some light on the issue by modeling the response of synoptic waves to both orography and ocean dynamics. Orographic forcing on eddies in the NH is concentrated over and downstream of the Tibetan Plateau, though ocean dynamics also influenced this region. This forcing slowed the eddy propagation speed, increasing its time in the baroclinic generation region in the Eastern Pacific Ocean. By comparison, the Rocky Mountains and the Alps had no influence, with transient eddies responding solely to ocean dynamics in the North American and European regions. Though these modeled influences show the climatological influences on storm tracks and do not reflect a change in climate, it could represent a starting point in determining the near-surface related causes of the 500 hPa undulance changes noted above.

In the SH, the continents of South America, South Africa, and Australia are each small in comparison to their regions. Of the SH regions, South America has the largest mountain range. Like the East Asian region, storm tracks are generally weak upstream and develop downstream of its mountain range (Trenberth 1991). Unlike the East Asian region, which has the least damped change in jet stream undulance at 500 hPa of the NH regions, the South American region has the most damped jet stream undulance of the SH regions. This complicates hypotheses regarding the relationship between changing atmospheric flow, orography and their effect on synoptic-scale wave genesis. Because

Wilson et al. (2009) only studied the NH, the relative impacts of orography and ocean currents in the SH are unknown.

4.3 Causes of jet undulation change

It is important to note the 500 hPa level lies at the base of the jet stream core. Because the greatest changes in jet undulation are ubiquitously observed in the upper troposphere, their primary cause is expected to lie in either direct upper tropospheric forcing or in stratospheric influences. The changes in undulation are likely related to the poleward shift in the jet streams. The poleward shifts have been dynamically linked to an increase in anticyclonic wave breaking (Rivière 2011) and larger wavelengths (Barnes and Hartmann 2011, Kidston et al., 2011). An increase in wave breaking would reveal itself as an increase in the frequency of highly undulated jet streams. These changes in undulation are then transferred downward into the middle troposphere. Though surface-related and lower tropospheric forcing will also influence the atmospheric flow in the middle troposphere, the primary sources of this forcing have yet to be determined.

The results of the study are inconsistent with expectations in light of the increase of zonal-mean zonal winds in the SH. Stronger zonal-mean zonal winds are expected to reduce the jet stream undulance. But if the poleward movement of the jet stream is caused by anticyclonic wave breaking and an increase in wavelength, it is likely their forcing is greater than that of an increase in the zonal-mean zonal wind.

From a global circulation perspective, an increase in jet stream undulance would provide the potential for stronger transient eddies and an intensified storm track. On the synoptic scale, the potential for an increase in the frequency of mature extratropical cyclones has large implications for the frequency of surface weather extremes.

5 FUTURE WORK

As discussed above, the cause of the changes in jet stream undulance remains to be seen. These changes need to be compared to other changes in the jet stream, such as its poleward movement and zonal-mean zonal wind speed changes, to determine their relationships. It is perhaps surprising that the changes in ratios over time, as seen in Figure 4, would be best represented by a linear trend. Instead, a second-degree parabolic function might be expected. While some regions include departures from the linear trend with decadal periodicity, the absence of these departures in all regions indicate they likely represent smaller regional influences. Thus, the trends in annual frequencies of symmetric ratios in each region could be compared with trends in carbon dioxide concentration, arctic sea ice extent and Arctic Amplification, tropical upper-tropospheric warming, and regional oscillation indices to determine their respective influences. In addition, all results above are noted as being qualitative and must be tested for their statistical significance.

6 REFERENCES

Arblaster, J. M., and G. A. Meehl, 2006: Contributions of external forcings to southern annular mode trends. *J. Climate*, **19**, 2896-2905.

Barnes, E. A., 2013: Revisiting the evidence linking arctic amplification to extreme weather in midlatitudes. *Geophys. Res. Letters*, **40**, 1-6, doi:10.1002/GRL.50880.

-------, and D. L. Hartmann, 2011: Rossby wave scales, propagation, and the variability of eddy-driven jets. *J. Atmos. Sciences*, **68**, 2893-2908.

-------, and L. Polvani, 2013: Response of the midlatitude jets, and of their variability, to increased greenhouse gases in the CMIP5 models. *J. Climate*, **26**, 7117-7135.

Chen, G., and I. M. Held, 2007: Phase speed spectra and the recent poleward shift of southern hemisphere surface westerlies. *Geophys. Res. Letters*, **34**, L21805, doi:10.1029/2007GL031200.

Ihara, C., and Y. Kushnir, 2009: Change of mean midlatitude westerlies in 21st century climate simulations. *Geophys. Res. Letters*, **36**, L13701, doi:10.1029/2009GL037674.

Kalnay, E., and Coauthors, 1996: The NCEP/NCAR 40-year reanalysis project, *Bull. Amer. Meteor. Soc.,* **77**, 437-471.

Kidston, J., G. K. Vallis, S. M. Dean, and J. A. Renwick, 2011: Can the increase in the eddy length scale under global warming cause the poleward shift of the jet streams? *J. Climate*, **24**, 3764-3780.

Laîné, A., M. Kageyama, D. Salas-Mélia, G. Ramstein, S. Planton, S. Denvil, and S. Tyteca, 2009: An energetics study of wintertime Northern Hemisphere storm tracks under 4 x CO_2 conditions in two ocean-atmosphere coupled models. *J. Climate*, **22**, 819-839.

Lorenz, D. J., and E. T. DeWeaver, 2007: Tropopause height and zonal wind response to global warming in the IPCC scenario integrations. *J. Geophys. Res.*, **112**, D10119, doi:10.1029/2006JD008087.

Miller, R. L., G. A. Schmidt, and D. T. Shindell, 2006: Forced annular variations in the 20th century Intergovernmental Panel on Climate Change Fourth Assessment Report models. *J. Geophys. Res.*, **111**, D18101, doi:10.1029/2005JD006323.

Rinke, A., and K. Dethloff, 2008: Simulated circum-Arctic climate changes by the end of the 21st century. *Global and Planetary Change*, **62**, 173-186.

Rivière, G., 2011: A dynamical interpretation of the poleward shift of the jet streams in global warming scenarios. *J. Atmos. Sciences*, **68**, 1253-1272.

Screen, J. A., and I. Simmonds, 2013: Exploring links between arctic amplification and mid-latitude weather. *Geophys. Res. Letters*, **40**, 959-964, doi:10.1002/GRL.50174.

Serreze, M. C., and R. G. Barry, 2011: Processes and impacts of arctic amplification: a research synthesis. *Global and Planetary Change*, **77**, 85-96.

Trenberth, K. E., 1991: Storm tracks in the southern hemisphere. *J. Atmos. Sciences*, **48**, 2159-2178.

Wilson, C., B. Sinha, and R. G. Williams, 2009: The effect of ocean dynamics and orography on atmospheric storm tracks. *J. Climate*, **22**, 3689-3702.

Woolings, T., and M. Blackburn, 2012: The north atlantic jet stream under climate change and its relation to the NAO and EA patterns. *J. Climate*, **25**, 886-902.

Yin, J. H., 2005: A consistent poleward shift of the storm tracks in simulations of 21st century climate. *Geophys. Res. Letters*, **32**, L18701, doi:10.1029/2005GL023684.

	North	South	West	East
N. America	70^o N	20^o N	150^o W	40^o W
Europe	70^o N	20^o N	40^o W	70^o E
E. Asia	70^o N	20^o N	60^o E	170^o E
Australia	20^o S	70^o S	90^o E	160^o W
S. Africa	20^o S	70^o S	30^o W	80^o E
S. America	20^o S	70^o S	115^o W	5^o W

Table 1 – The northern, southern, western, and eastern extents of the six regions of interest.

	250 hPa	500 hPa	250 hpa / 500 hPa
N America	3.28	0.43*	7.6*
Europe	2.58	-0.13*	-20.6*
E Asia	3.11	2.25	1.4
S America	5.13	1.71	3.0
S Africa	6.49	3.14	2.1
Australia	5.41	3.19	1.7

Table 2 - The sum of the change of all ratios greater than the median symmetric ratio at 250 hPa and 500 hPa. The sums indicate the cumulative linear change in the frequency of symmetric ratios from relatively zonal to meridional patterns for each year of the dataset. Negative sums indicate a net decrease in jet stream undulance. The ratio of 250 hPa to 500 hPa sums shows the damping effects between the two pressure levels.

*Although sums of ratio change are calculated, these regions lack of a qualitative pattern of change in undulation. Their computed damping effects should be interpreted accordingly.

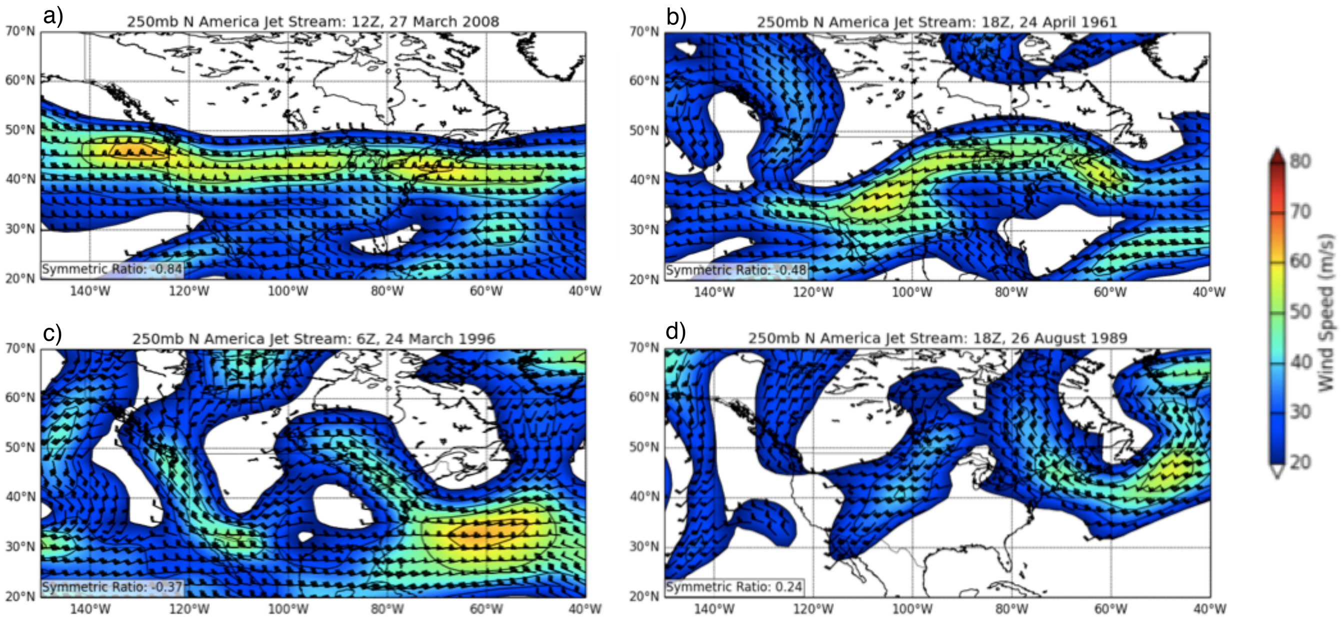

Figure 1 – Vector winds at 250 hPa greater than 20 ms^{-1} (barbs; pennants indicate 50 ms^{-1}, full barbs 10 ms^{-1}, half barbs 5 ms^{-1}) and wind speed (ms^{-1}; filled) for N. America region. (a) The minimum symmetric ratio in the region at 250 hPa in the 1948-2013 time period is -0.84 and occurs at 12 UTC, 27 March 2008. (b) The median symmetric ratio is -0.48 occurs at 18 UTC, 24 April 1961. (c) The nearest symmetric ratio to the mean is -0.37 occurs at 6 UTC, 24 March 1996. (d) The maximum symmetric ratio is 0.24 occurs at 18 UTC, 26 August 1989.

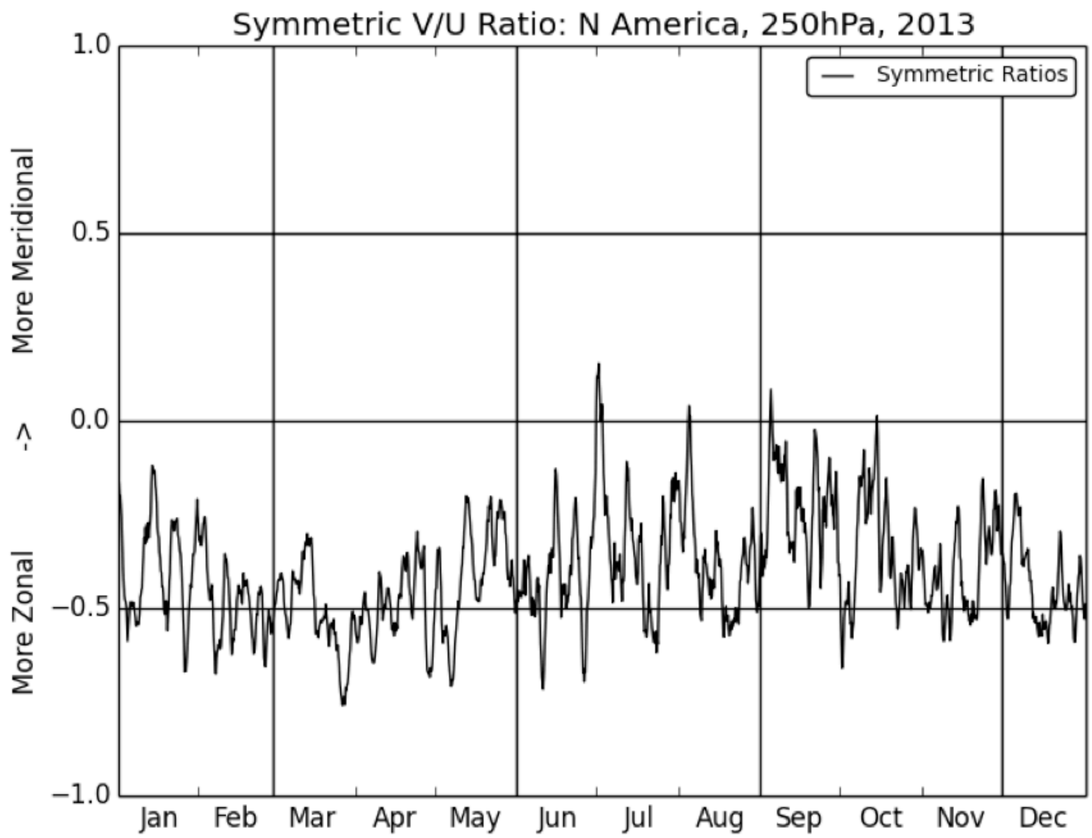

Figure 2 – An example time series of symmetric ratios vs. time at 250 hPa in the N. America region for 2013. Symmetric ratios are calculated 4x daily at 00 UTC, 06 UTC, 12 UTC, and 18 UTC. Similar time series can be produced for any region, year, and pressure level.

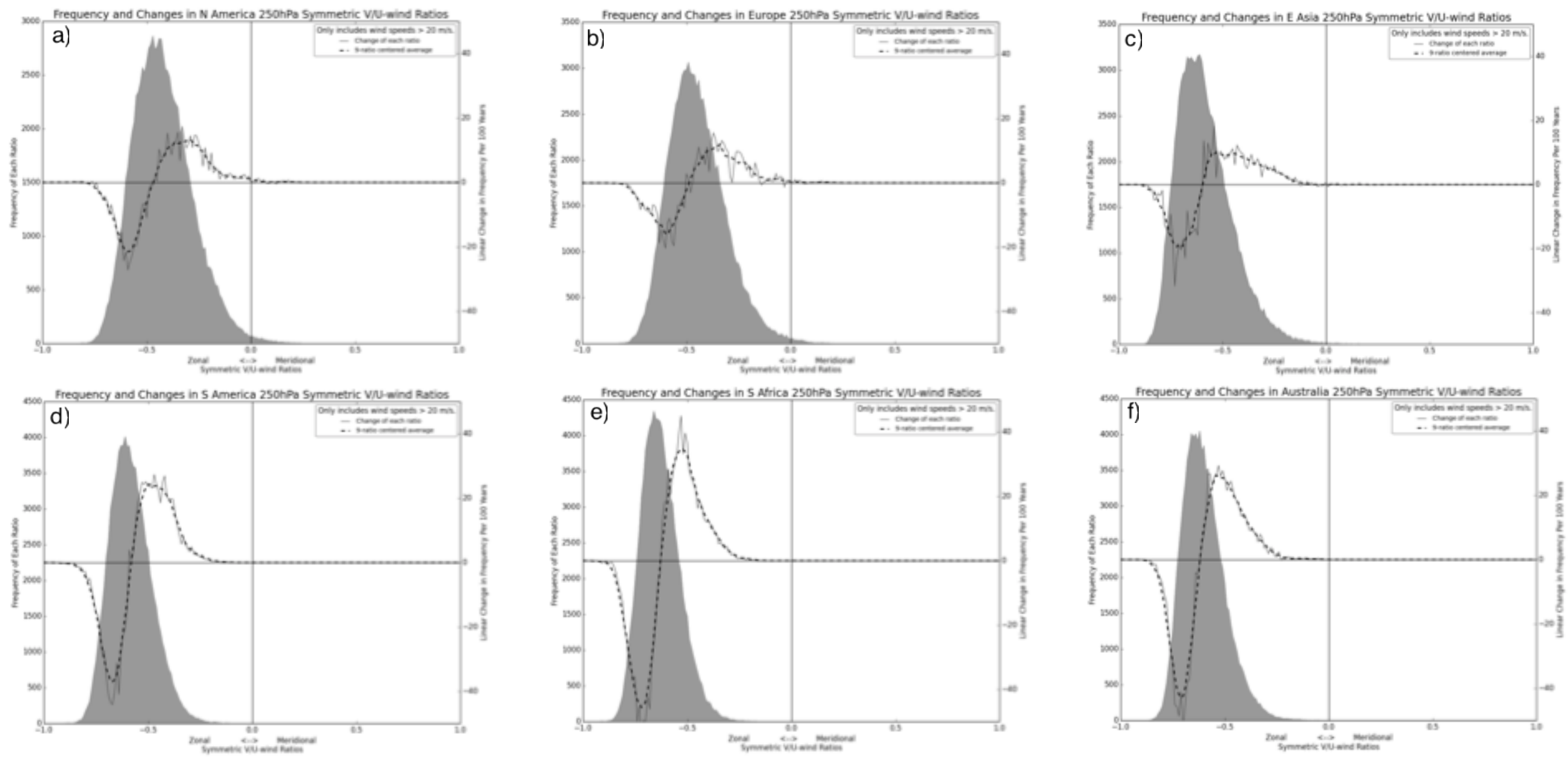

Figure 3 – Histogram of symmetric ratio frequencies for 1948-2013 (gray fill, left vertical axis), linear rate of change in symmetric ratio frequency per 100 years (thin solid line, right vertical axis), and 9-ratio centered average of linear rate of frequency change per 100 years (bold dashed line, right vertical axis) at 250 hPa for (a) N. America, (b) Europe, (c) E. Asia, (d) S. America, (e) S. Africa, and (f) Australia.

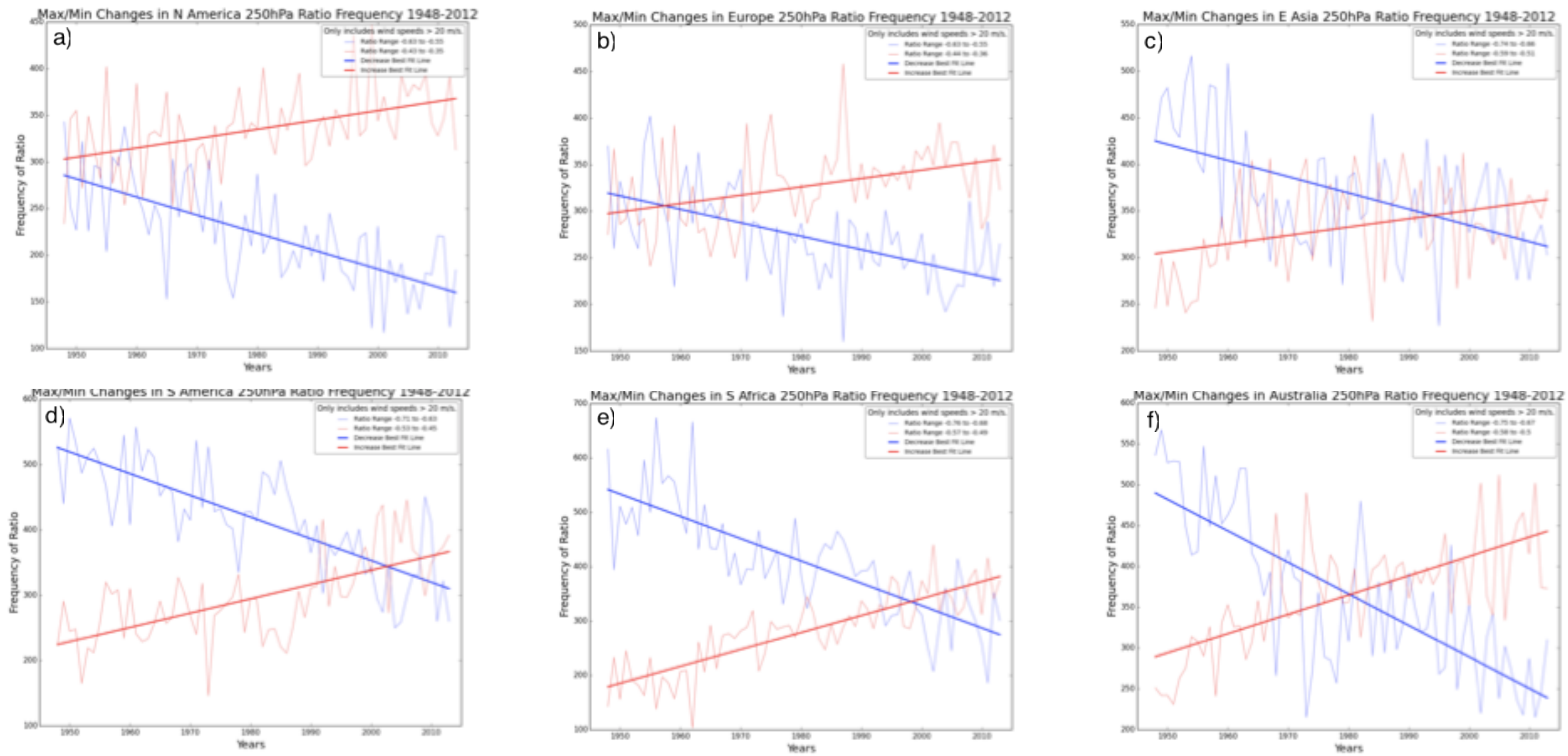

Figure 4 – The largest increasing (red) and decreasing (blue) linear rate of change in the 9-symmetric ratio centered average at 250 hPa is found. The sum of the frequencies for the nine ratios (thin line) and their linear regression line (bold line) are plotted by year. (a) N. America, (b) Europe, (c) E. Asia, (d) S. America, (e) S. Africa, and (f) Australia regions.

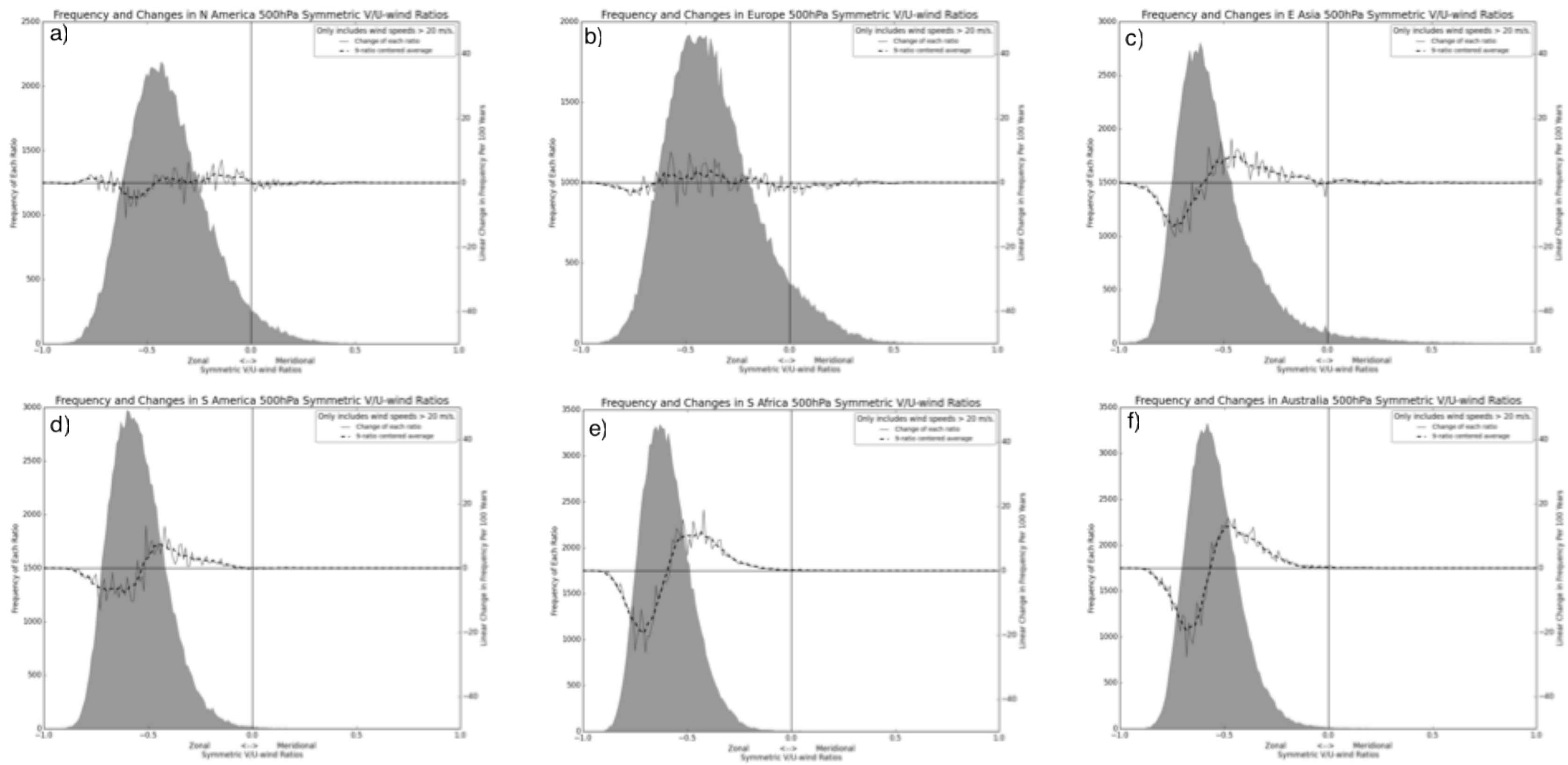

Figure 5 – As in Figure 3, but for 500 hPa.

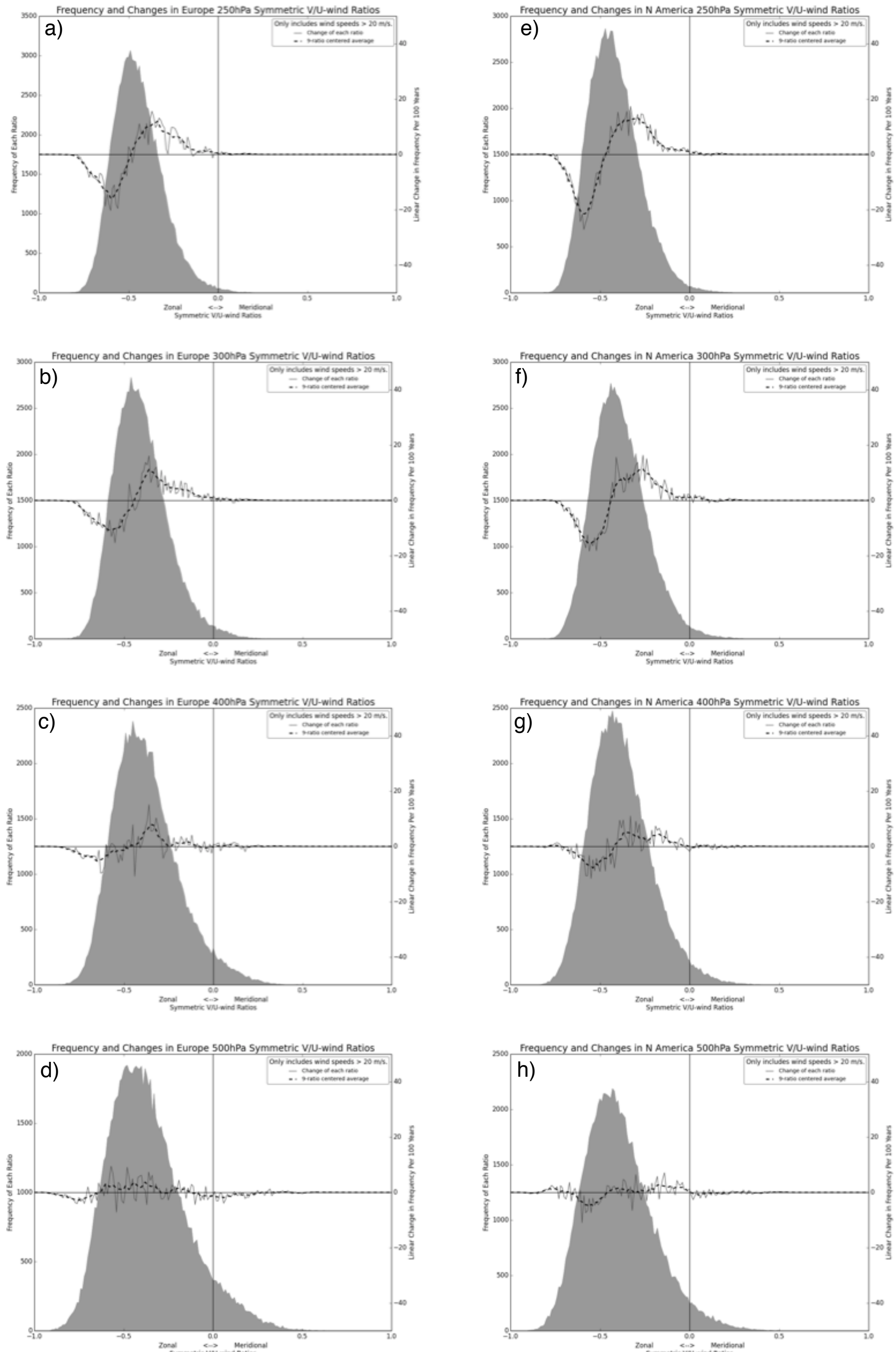

Figure 6 – As in figure 3, but (a-d) is N American region, (e-h) is Europe region. Pressure levels plotted: (a, e) is 250 hPa, (b, f) is 300 hPa, (c, g) is 400 hPa, and (d, h) is 500 hPa.